Int. J. Rock Mech. Min. Sci. & Geomech. Abstr. Vol.30, No.7, pp. 1311–1317, 1993
Printed in Great Britain

0148-9062/93 $6.00 + 0.00
Pergamon Press Ltd

Influence of Rock Joint Degradation on Hydraulic Conductivity

M. J. BOULON *
A. P. S. SELVADURAI †
H. BENJELLOUN ‡
B. FEUGA §

This paper presents experimental results for hydraulic conductivity of rock joints (granite) under normal load without shearing or after shear displacements. A meso-scale model describing the flow changes, locally based on the cubic law, and taking into account the asperity degradation is proposed. This model uses two constitutive parameters and assumes that the change in maximum hydraulic opening and in normal relative displacement are the same. The tests mentioned hereabove are analysed by this model which shows a reasonable capacity of simulation and gives the maximum Reynolds number of the flow.

INTRODUCTION

The flow of water in fractured geological media has important applications to the design and construction of mines, dams, oil and gas reservoirs, and environmental geotechnique. The hydraulic conductivity of rock joints in particular has been investigated by many authors utilizing various approaches. The earlier treatment of hydraulic conductivity of fractured rock masses has largely focussed on the evaluation of their bulk hydraulic conductivity (Baker [1], Braester [2], Lomize [3]). Later developments involving statistical and stochastic methods take into consideration complex flow processes in fractured networks (Andersson et al [4], Cacas et al [5], Hestir et al [6], Long et al [7]). These developments largely focussed on the evaluation of the hydraulic conductivity of fractured rock masses where the fracture network is not influenced by the flow process or changes in the geostatic state of stress. In situations involving stress relief, such as problems associated with underground excavations and tunneling, loads imposed by dam construction etc, the hydraulic conductivity characteristics of preexisting fractures can be altered by the relative movements both tangential and normal at the faces of the fracture (Pine and Batchelor [8]). These movements modify the global hydraulic conductivity of the rockmass by changing the geometry of the flow regions. It is well known that dilatancy and asperity degradation can modify the flow characteristics (Barton et al [9], Bandis et al [10], Teufel [11], Makurat et al [12]). Laboratory tests on fractured samples undergoing changes in normal stress have highlighted the scale effect (Gale [13], Gentier [14], Kranz et al [15], Walsh [16]). The experimentation also included the important influence of either the morphology of the rock walls (Elsworth and Goodman [17], Engelder and Scholz [18], Walsh [16]), or the distribution of void space (Billaux and Gentier [19], Tsang and Witherspoon [20] on the hydraulic conductivity of joints. In contrast, there are relatively few investigations which examine the role of the shear of a fracture on its hydraulic conductivity (Bandis et al [10], Teufel [11], Makurat et al [12], Barton et al [9]). Many authors employ a corrective factor which allows for the coupling between the mechanical and the hydraulic aspects of the aperture. Asperity degradation due to shearing and the resulting changes in hydraulic aperture seem to be much more difficult to model than those primarily due to normal joint displacements. The reliability of the predictions probably depend both on experimental factors such as the quality of the experiments (presence or absence of joint wall rotations), and on the intrinsic predictive capability of the Hele-Shaw (cubic law) model completed (or not) by a joint degradation appraisal. Previous investigations deal with either a macro-scale analysis (Barton et al [9], Bandis et al [10]) or with a micro-scale approach (Billaux and Gentier [19]). The first part of this paper deals with original 2D hydraulic conductivity experiments performed on rock joints subjected both to normal loads without shearing and to normal loads after shear displacements. These experiments were carried out at the BRGM (Benjelloun [21]). The subsequent analysis is based on a meso-scale model applied to simulating these tests. It does not involve a mechanical analysis resulting from an interface constitutive equation (Benjelloun et al [22]). In our hydraulic interpretation asperity degradation itself is not calculated but its influence on hydraulic conductivity is taken into account through the

* Laboratoire 3S, University Joseph Fourier, Grenoble, France
† Department of Civil and Environmental Engineering, Carleton University, Ottawa, Canada
‡ Formerly Bureau de Recherches Géologiques et Minières (BRGM), Orléans, France. Presently Société Géodia, Paris, France
§ BRGM, Orléans, France and Ecole des Mines, Nancy, France

joint normal displacement. The originality of this method is based on a direct link (without any correcting factor) between the normal displacement and the change in the distribution of hydraulic apertures. As this approach was tested for a small number of samples, its application to real situations is evaluated.

EXPERIMENTAL DEVICE AND TESTS

Hydraulic conductivity tests were conducted on natural and artificial (hydraulic fracture) 15cm*15cm rock joint samples saturated by water, under normal loads without shear displacement or after shear displacement -Fig. 1a-. The geometry of the flow was prescribed to be 1D at the macro-

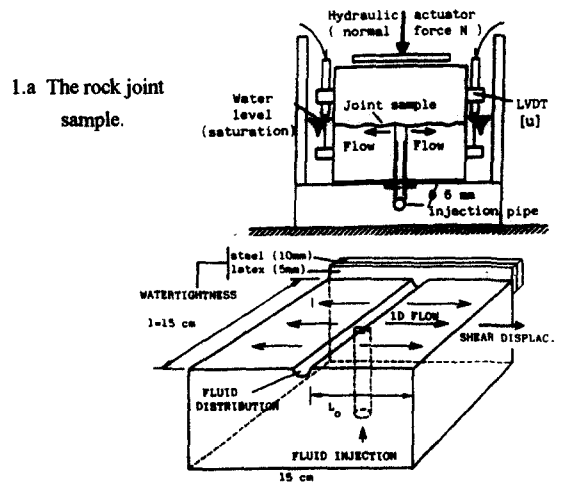

1.a The rock joint sample.

1b. The rock joint sample prepared for a 1D flow.

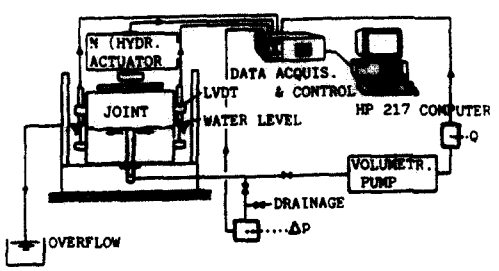

1c. The measurement and acquisition system.

Fig. 1. Experimental device for hydraulic conductivity measurements.

scopic scale by using two lateral watertightness plates (steel and latex membrane) -Fig. 1b-. A volumetric pump and a needle valve provided a stable fluid flow during the experiments -Fig. 1c-. The data acquisition and control unit and the micro-computer allowed control and measurement of the normal force N, the normal relative displacement [u], the shear displacement [w], the fluid flow Q and its pressure Δp (hydraulic head ΔH). One should note that the shear force was not measured during these tests (prescribed shear displacement). For every test the sample was saturated and a light cyclic preload was applied in order to fit the rock walls together before the conductivity experiment itself. According to Fig. 1.b we will denote by L_0 and 2l the macroscopic initial (before shearing) lengths along and perpendicular to the flow direction respectively.

Tests under normal stress

Two typical rock joints were investigated: an artificial (by hydraulic fracturation) rough fracture L2 (Lanhelin granite) and a natural weathered rough fracture G16 (Guéret granite). Their physical and mechanical characteristics are

Sample	Lanhelin (L1,L2)	Gueret (G16)
JRC*	13-15	18-20
Young mod. (Mpa)	59000	68000
Comp. Strength (Mpa)	90	180
P-Wave Veloc. (m/s)	5600	6000

Tab. 1. Main physical and mechanical properties of granite samples L1/L2 (Lanhelin, Brittany, France) and G16 (Gueret, French Massif Central).

summarized in Tab. 1. Figure 2 shows a typical experimental sequence for the joint sample L2: the changes

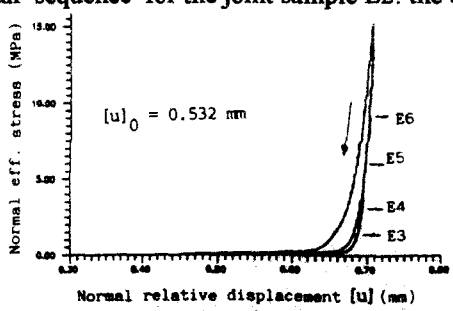

Fig. 2. Typical experimental sequence of conductivity tests (E3, E4, E5, E6) for joint L2 .

in normal relative displacement (increasing corresponds to joint closure) associated with the variations of effective stress and the stress levels E3 to E6 corresponding to the conductivity tests. The preload cycles are also presented . During the tests, the hydraulic flow was progressively increased (step by step), controlled and limited in order to correspond to the linear part of the Q-ΔH curve of the joint, which allows for a better comparison of the set of tests. A tentative evaluation of the joint degradation due to this history can be measured by the hysteresis surface on Fig. 2 (Plesha [23], Benjelloun et al [22]). The mechanical and hydraulic data for these tests are presented in Tables 2 and 3. The ratio of hydraulic conductivity between high (up to 22 MPa -sample G16-) and low stress is in the range of 1/10.

Test	σ_n (MPa)	[u] (mm)	Q/ΔH (m^2/s)
E3	1.39	0.147	5.90e-8
E4	3.64	0.154	1.98e-8
E5	5.95	0.159	1.04e-8
E6	9.14	0.160	5.19e-9

Tab. 2. Mechanical and hydraulic data of conductivity tests on sample L2 (l_o = 11 cm, L_o = 7 cm).

* evaluated by profile morphology and mechanical measurements prior to shearing

Test	σ_n (MPa)	[u] (mm)	Q/ΔH (m^2/s)
E1	2.40	0.052	2.89e-6
E2	7.08	0.067	1.14e-6
E3	11.9	0.074	9.27e-7
E4	16.7	0.079	7.57e-7
E5	22.3	0.082	5.83e-7

Tab. 3. Mechanical and hydraulic data of conductivity tests on sample G16 (l_o = 15 cm, L_o = 7 cm).

Shearing tests

Measuring the joint conductivity during shearing represents an important scientific challenge involving complex devices (Makurat et al [12]). We separately investigated the evaluation of the degradation due to the shearing under high stress (influencing the hydraulic conductivity) and the calculation of the hydraulic conductivity for a known normal relative displacement of the joint walls. In this paper we assume that the rock joint constitutive equation is able to provide the normal displacement [u] for any loading history of the joint. The present experiments then consist of normal loadings of the joints after shearing under zero normal stress. Consequently the degradation due to a real shear (under high normal stress) is not taken into account. The hydraulic conductivity of two typical rock joints is presented: an artificial rough fracture L1 (Lanhelin granite) and the previous natural weathered rough fracture G16. Their physical and mechanical characteristics are given in Tab. 1. The roughness of sample G16 in its state after normal loading should has been reduced. It has not been measured. Fig. 3 shows a typical experimental sequence for the joint G16: the changes in normal relative displacement (decrease

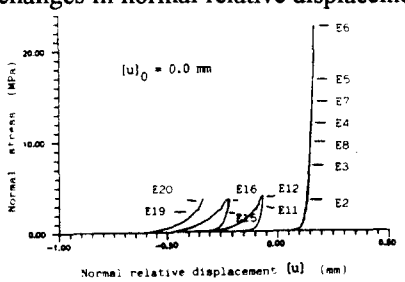

3.a. Normal stress versus Normal relative displacement.

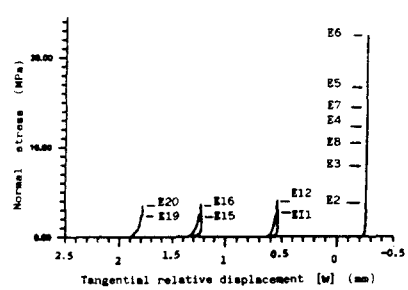

3.b. Normal stress versus Tangential relative displacement.

Fig.3. Typical experimental sequence of conductivity tests (E2, E3, ..., E19, E20) for joint G16 under shearing.

means joint opening) and the corresponding tangential relative displacements [w] associated with the variations of effective stress and the stress levels corresponding to the conductivity tests. The mechanical and hydraulic data of these tests are presented in Tab. 4 and 5. Here, due to the joint dilatancy the ratio of conductivity between tests involving shearing or without it is in the range 1/10000. Fig. 3 shows that the degradation effect during a cycle (increasing function of the surface of the hysteresis loop in

Test	σ_n (MPa)	[u] (mm)	[w] (mm)	Q/ΔH (m^2/s)
E2	6.37	0.260	0.081	4.94e-8
E3	2.54	0.245	0.082	1.40e-7
E5	2.55	0.065	0.524	1.55e-5
E6	3.32	0.086	0.511	0.70e-6
E7	0.69	0.076	0.52	0.77e-6
E9	0.64	-0.386	1.13	3.46e-4
E10	1.31	-0.318	1.11	2.96e-4
E11	1.67	-0.286	1.09	2.57e-4
E12	2.06	-0.262	1.08	2.29e-4
E14	2.26	-0.108	0.79	8.85e-5
E16	0.72	-0.136	0.81	9.04e-5
E17	1.64	-0.110	0.8	7.80e-5
E18	2.51	-0.096	0.78	7.55e-5

Tab. 4. Mechanical and hydraulic data of conductivity tests on sample L1 (l_o = 15 cm, L_o = 7 cm).

Test	σ_n (MPa)	[u] (mm)	[w] (mm)	Q/ΔH (m^2/s)
E2	3.43	0.127	-0.226	2.96e-6
E3	7.21	0.142	-0.228	1.17e-6
E4	12.0	0.149	-0.230	9.34e-7
E5	16.7	0.154	-0.232	7.70e-7
E6	22.4	0.157	-0.233	5.93e-7
E7	14.3	0.153	-0.233	6.95e-7
E8	9.77	0.148	-0.232	7.32e-7
E11	2.93	-0.088	0.555	7.70e-5
E12	3.93	-0.070	0.555	7.46e-5
E15	2.44	-0.251	1.249	3.05e-4
E16	3.61	-0.220	1.249	2.15e-4
E19	2.45	-0.355	1.823	4.50e-4
E20	3.53	-0.328	1.801	4.34e-4

Tab. 5. Mechanical and hydraulic data of conductivity tests on sample G16 (l_o = 15 cm, L_o = 7 cm).

the σ_n-[u] plane) is larger when fresh contacts are involved (after tangential displacement).

MODELLING THE FLOW CHANGES

Basic modelling in the literature

As mechanical measurements only record the normal displacement [u] between the joint walls, there is a basic difficulty for calculating the macroscopic 1D flow Q through a joint. The well known cubic law (Gale et al [13]), based on

the analogy between the real flow and a viscous flow of thickness e_h (e_h being the equivalent hydraulic aperture) passing through two parallel plates is the most used model in the literature. It assumes a small enough Reynolds number for the flow. The highly non linear relationship between [u] and e_h is complicated by the presence of infill materials. The ratio between the conducting aperture and the mechanical aperture e_m has been found to decrease when the normal stress level increases. Barton et al [9] proposed an empirical relation linking these two parameters and JRC_o, initial value of JRC.

$$e_h = (e_m)^2 / (JRC_o)^{2.5} \quad (1)$$

But the evaluation of e_m needs the definition of its origin which remains subjective, and the JRC coefficient itself results from correlations involving an inherent scatter.

Principles of a meso-scale model

The main features and assumptions of our meso-scale model are:

(i) An initial distribution of e_h (from zero to a maximum value e_{hmo}) is assumed within the joint before any loading. An exhaustive sampling of the channel thicknesses shows a ratio y of thickness less than e_h. This distribution obeys the power law -Fig. 4a-:

$$e_h = y^n e_{hmo} \quad (2)$$

(ii) The change in that distribution is directly linked to the change in [u] which is measurable, provided that there is no joint wall rotation during the experiment. This assumption is valid for small relative displacements -Fig. 4b-.

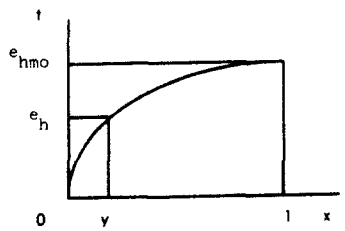

4.a. Initial distribution of e_h

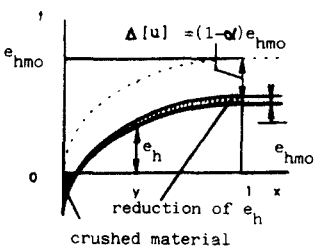

4.b. Change in e_h due to change in [u] without change in [w]

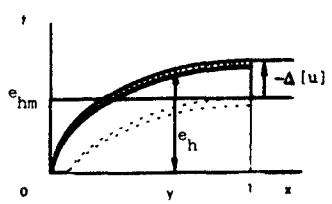

4.c. Change in e_h due to change [u] with change in [w].

Fig. 4. Meso-scale model of rock joint hydraulic conductivity: principles.

$$de_h = -d[u] \quad \text{if} \quad e_h > -d[u] \quad (3)$$

(iii) The degradation of the joint asperities is modelled by irreversible changes in e_h. Due to changes in [u] without variation of [w] the thickness of certain channels can vanish. Then the equivalent volume of material is assumed to remain within the joint and to uniformly reduce the thickness of open channels - Fig. 4b-.

(iv) The joint is considered as a set of independent parallel plates whose individual spacing is e_h, whose length is L (updated value of L_o taking into account changes in [w]) and whose width is the fraction 2dl = 2ldy referring to the distribution of e_h). According to the cubic law the corresponding contribution to the global flow is:

$$d\left(\frac{Q}{\Delta H}\right) = \frac{\rho g}{12\mu L} e_h^3 \; 2ldy = \frac{\rho g}{6\mu L} e_h^3 \; ldy \quad (4)$$

(ρ : mass density of the fluid, g : acceleration due to gravity and μ : dynamic viscosity of the fluid)

(v) The global flow is then:

$$\frac{Q}{\Delta H} = \int_{joint} \frac{\rho g l}{6\mu L} e_h^3 \, dy \quad (5)$$

(vi) When shear displacements occur, the distribution of e_h is updated according to the new value of [u] (dilation), to the volume of joint material previously degraded, and to a the minimum value of e_h being equal to zero (provided than σ_n has a positive value).

Formulations derived from these principles

The global rate of flow per unit hydraulic head passing through the joint can be calculated analytically. In the initial situation (previously unloaded joint, $\sigma_n = 0$):

$$\frac{Q}{\Delta H} = \frac{1}{3n+1} \frac{\rho g l \, e_{hmo}^3}{6\mu L} \quad (6)$$

Let us use the parameter β:

$$\beta = 1 - \alpha \quad (7)$$

After a joint closure $-\Delta[u] = \alpha e_{hmo}$ without any tangential displacement ($0 < \alpha < 1$ according to Fig. 4.b) the flow is reduced to the following:

$$\frac{Q}{\Delta H} = \frac{\rho g l \, e_{hmo}^3}{6\mu L} \left[\frac{1}{3n+1} - \frac{3\beta}{2n+1} + \frac{3\beta^2}{n+1} - \beta^3 - \beta^{1+\frac{1}{n}} \left(\frac{1}{3n+1} - \frac{3}{2n+1} + \frac{3}{n+1} - 1 \right) \right] \quad (8)$$

As shown in Fig. 4.b the uniform channel thickness reduction acts as a modification $\Delta\alpha$ in the parameter α:

$$\Delta\alpha = - \frac{n\beta^{1+\frac{1}{n}}}{(n+1)(1-\beta^{\frac{1}{n}})} \qquad (9)$$

After a shear displacement corresponding to a joint aperture (due to dilation) or to a large negative change in [u]:

$$\Delta[u] = (1-\alpha)\, e_{hm} \qquad (\alpha > 1) \qquad (10)$$

the former rate of flow / unit hydraulic head is magnified by the following function:

$$\left(\frac{\alpha + \Delta\alpha}{1 + \Delta\alpha}\right)^3 \qquad (11)$$

This model only has two independent parameters which need to be determined for any joint loading history: e_{hmo} controlling the initial size of the set of channels, and n characterizing the initial shape of the voids within the joint. One can choose to identify these parameters either after the whole set of hydraulic tests or after only some limited tests.

INTERPRETATION OF THE CONDUCTIVITY EXPERIMENTS

Basic results

Fig. 5 to 8 summarize the results obtained for the four sets of experiments detailed in Tables 2 to 5. For each joint a basic simulation has been made by the cubic law identified from the first conductivity experiment (giving a first evaluation of the hydraulic aperture). The further points of the simulation assume the same change for the mechanical and for the hydraulic aperture. For the meso-scale model we identified the constitutive parameters by minimizing the deviation between experience and simulation, taking into account the assumption (ii) and the whole set of experiments related to each joint. This deviation is represented by the arithmetic mean value of the residuals related to each conductivity test.

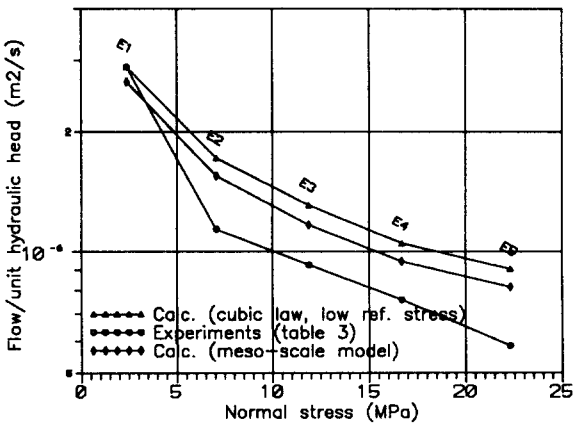

Fig.6. Sample G16 under normal stress, hydraulic conductivity experiments and simulations. Meso-scale model: n = 0.09, e_{hmo} = 0.165 mm, mean residual = 2e-7 m^2/s.

Discussion of the simulation results

The meso-scale model generally exhibits a smaller deviation from the experience (typical range: 0 - 40%) than the cubic law (typical range: 0 - 100%). It better follows the different changes in hydraulic conductivity , which indicates that the degradation effect really has to be taken into account. From an hydraulic point of view, the Reynolds number related to the classical cubic law has a limited meaning since the opening aperture represents a mean value without a knowledge of the maximum value. For the meso-scale model

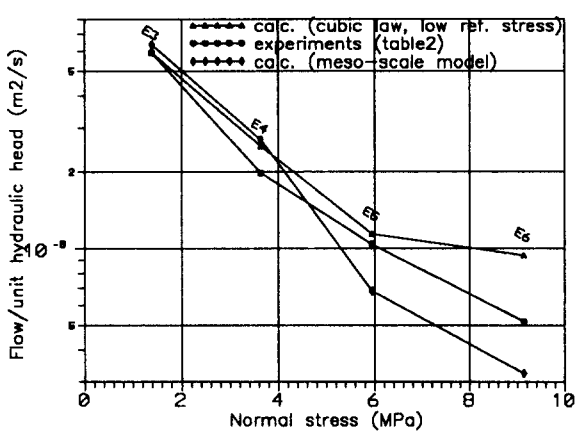

Fig.5. Sample L2 under normal stress, conductivity experiments and simulations. Meso-scale model: n = 0.21, e_{hmo} = 0.207 mm, mean residual = 4e-9 m^2/s.

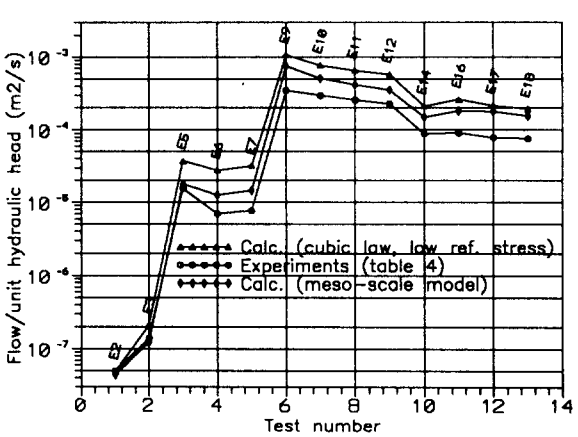

Fig.7. Sample L1 under shear displacements and normal stress, conductivity experiments and simulations. Meso-scale model: n = 0.07, e_{hmo} = 0.297 mm, mean residual = 7e-5 m^2/s.

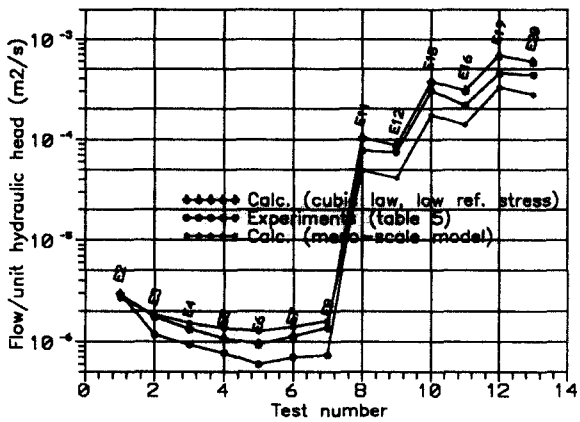

Fig.8. Sample G16 under shear displacements and normal stress, hydraulic conductivity experiments and simulations. Meso-scale model: n = 0.30, e_{hmo} = 0.270 mm, mean residual = 3e-5 m^2/s

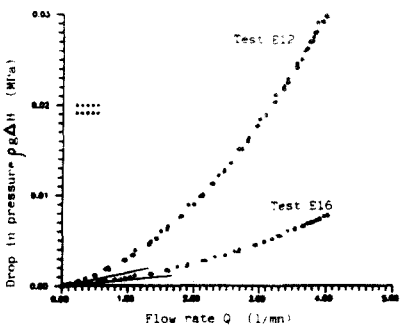

Fig. 9. Hydraulic behaviour of the joint sample G16 under various flow rates (Experiments described in Table 5)

e_{hm} represents the maximum value of the opening aperture within the joint. Then we can calculate the maximum Reynolds number related to every conductivity test (Tab. 6). From this point of view, the tests involving a large flow show a large Reynolds number which contradicts the local cubic law assumption. The non linearity of the Q-ΔH curve characterizing a joint is well known (Figure 9). For this reason an interpretation by the global cubic law or by our meso-scale model (using a local cubic law) only has a sense for the initial slope of the Q-ΔH curves.

Test	Re	Test	Re	Test	Re	Test	Re	Test	Re
samp. L2		E2	15	E7	285	*samp. G16*		E15	129
under		E3	14	E9	9.5	*under*		E16	153
norm. str.		E4	14	E10	196	*shear displ.*		E19	156
E3	43	E5	16	E11	187	E2	226	E20	142
E4	73			E12	183	E3	419		
E5	84	*samp. L1*		E14	192	E4	455		
E6	150	*under*		E16	230	E5	498		
		shear displ.		E17	250	E6	608		
samp. G16		E2	220	E18	227	E7	576		
under		E3	216			E8	620		
norm. str.		E5	165			E11	158		
E1	9.5	E6	272			E12	142		

Tab. 6. Maximum Reynolds numbers during hydraulic conductivity tests (meso-scale model).

Physical meaning of the parameters n and e_{hmo}

The maximum hydraulic aperture e_{hmo} before joint loading does not need any further explanation. The exponent n (power law) allows to describe roughly the structure of the voids within the joint:

high n (0.3) ⇔ smooth joint walls and thin channels
small n (<0.1) ⇔ rough joint walls and thick channels

From a probabilistic point of view the distribution mentioned at item (i) corresponds to a off centered repartition of mean value $\bar{e}$ and of standard deviation $\bar{\sigma}$:

$$\bar{e} = \frac{e_{hmo}}{n+1}$$

$$\bar{\sigma} = \frac{n}{(n+1)\sqrt{2n+1}}\, e_{hmo} \qquad (12)$$

Since the roughness can't be in itself a measure of the void repartition, we can remark that the sample L2 (Fig. 5), artificial fracture subjected to an intense cyclic preloading, has a high value of n and corresponds to a medium roughness. On the other hand the sample G16 (natural weathered fracture) under normal stress (Fig. 6) has a small value of n, as well as sample L1 (Fig. 7), identical to L2 before cyclic preloading. The first loading (Fig. 6), which makes the fracture walls smoother, allows a high value of n at the beginning of the shear test for sample G16 (Fig. 8).

APPLICATION TO REAL SITUATIONS

Other validation tests obviously are still necessary for assessing the predictive capacity of this meso-scale model. The investigation of the hydraulic conductivity of a new rock joint needs some loadings in terms of normal stress in order to identify the initial maximum hydraulic aperture e_{hmo} and the coefficient n characterizing the proportion of small and large channels.

CONCLUSIONS

This model of rock joint hydraulic conductivity describes the changes in the distribution of apertures associated to changes in normal stress inducing an asperity degradation and to changes in shear displacements. This hydraulic model has to be associated with a mechanical constitutive model for a complete efficiency. For this model it is possible to follow

the changes in channel thickness related to a loading history and to control the validity of the local cubic law through the maximum Reynolds number related to a conductivity test.

REFERENCES

1. Baker W. J. Flow in fissured formations. *Proc. of the fourth Petroleum Congress, Rome* **V.II**, 379-393 (1955).
2. Braester C. Discrete and continuum approaches to solution of flow problems in fractured rocks. *Proc. of the Fourth Canadian/American Conf. on Hydrogeology - Fluid flow, heat transfer and mass transport in fractured rocks.* Banff, Alberta, Canada, Alta. Res. C. and N.W.W.A., 223-229 (1988).
3. Lomize G. M. *Flow in fractured media* (in Russian), p. 127. Gosenergoizdat ,Moscow (1951).
4. Andersson J. Shapiro A. M. and Bear J. A stochastic model of a fractured rock conditioned by measured information. *Water Resources Res.* **20** (1), 79-88 (1984).
5. Cacas M. C., Ledoux E., de Marsily G., Tillie B., Barbreau A., Durand D., Feuga B. and Peaudecerf P. Modeling fracture flow with a stochastic discrete fracture network: calibration and validation. 1: The flow model *Water Resources Res.* **26** (3), 479-489 (1990).
6. Hestir K., Long J. C. S., Chilès J. P. and Billaux D. Some techniques for stochastic modeling of three dimensional fracture networks. *Geostatistical sensitivity and uncertainty methods for groundwater flow and radionuclide tranport modeling.* B. E. Buxton Ed., Battelle Press, Columbus, Ohio, USA, 495-519 (1989).
7. Long J. C. S., Gilmour P. and Witherspoon P. A. A model for steady fluid flow in random three-dimensional networks of disc-shaped fractures. *Water Resources Res.*, **18** (3), 1105-1115 (1985).
8. Pine R. J. and Batchelor A. S. Downward migration of shearing in jointed rock during hydraulic injections, *Int. J. Rock Mech. Min. Sci. & Geomech. Abstr.* **21**, 5, 249-263 (1984).
9. Barton N., Bandis S. and Bakhtar K. Strength Deformation and Conductivity of rock joints. *Int. J. Rock Mech. Min. Sci. & Geomech. Abstr.* **22**, 3, 121-140 (1985).
10. Bandis S. C., Makurat A. and Nik G. Predicted and measured hydraulic conductivity of rock joints. *Proc. of the Int. Symp. on Fundamentals of Rock Joints* Björkliden , Norway (1985).
11. Teufel L. W. Permeability changes during shear deformation of fractured rock. *28th US Symp. on Rock Mech.*, Tucson USA (1987).
12. Makurat A., Barton N., Rad N. S. and Bandis, S. C. Joint conductivity variation due to normal and shear deformation, *Proc. of the Int. Symp. on Rock joints* Loen, Norway, Balkema ed. Rotterdam, The Netherlands, 535-540 (1990).
13. Gale J. E. and Raven K. G. Effects of sample size on the stress-permeability relationship for natural fractures, *Technical information report nr. 48*, dept. of earth sciences, University of Waterloo, Ontario, Canada (1980).
14. Gentier S. Morphologie et comportement hydromécanique d'une fracture naturelle dans le granite sous contrainte normale - Etude expérimentale et théorique, *Thèse de Doctorat*, Université d'Orléans, France (1986).
15. Kranz R. L., Frankel A. D., Engelder T. and Scholz C. H. The permeability of whole and jointed Berre granite *Int. J. Rock Mech. Min. Sci. & Geomech. Abstr.* **16**, 225-234 (1979).
16. Walsh J. B. Effect of pore pressure and confining pressure on fracture permeability. *Int. J. Rock Mech. Min. Sci. & Geomech. Abstr.* **18**, 429-435 (1981)
17. Elsworth D. and Goodman R. E. Hydro-mechanical characterization of rock fissures of idealized sawtooth or sinusoidal form *Proc. of the Int. symp. on Fundamentals of Rock Joints* Björkliden , Norway (1985).
18. Engelder T. and Scholz C. H. Fluid flow along very smooth joints at effective pressure up to 200 Megapascal, *Amer. Geophys. Union monograph* nr 25, (1981).
19. Billaux D. and Gentier S. Numerical and laboratory studies of flow in a fracture. *Proc. of the Int. Symp. on Rock Joints* Loen, Norway, Balkema ed. Rotterdam, The Netherlands, 369-374 (1990).
20. Tsang Y. W. and Witherspoon P. A. Correlations between fracture roughness characteristics and fracture mechanical and fluid flow properties *23th US Symp. on Rock Mechanics* Berkeley, USA, *Issues in Rock Mechanics, chapt. 58.* 560-567 (1982).
21. Benjelloun, Z. H. (1991), Contribution à l'étude experimentale et numérique du comportement mécanique et hydraulique des joints rocheux, Thesis, BRGM and University Joseph Fourier, Grenoble, France
22. Benjelloun Z. H., Boulon M. and Billaux D. Experimental and numerical investigation on rock joints. *Proc. of the Int. Symp. on Rock Joints* Loen, Norway, Balkema ed. Rotterdam, The Netherlands, 171-178 (1990).
23. Plesha M.E. Constitutive models for rock discontinuities with dilatancy and surface degradation. *Int. J. Num. Anal. Meth. Geomech.*, **11**, 345 - 362 (1987).